JOURNAL OF APPLIED ELECTROCHEMISTRY 13 (1983) 473–487

Water desalting by means of electrochemical parametric pumping. I. The equilibrium properties of a batch unit cell

Y. OREN, A. SOFFER

Nuclear Research Center, Negev, Beer Sheva, POB 9001, Israel, 84190

Received 20 April 1982; revised 20 October 1982

It was shown previously that adsorption of ions at the electrical double layer of a high specific surface area carbon electrode can serve for water desalination. This is effected by assembling two such electrodes in a cell, cycling electronic charge between them and applying periodic synchronous pumping of the liquid through the cell. This process has been termed Electrochemical Parametric Pumping (ECPP). In the present article, modified charge coordinates, desalting efficiencies, isopotentiograms (analogous to adsorption isotherms) and optimization considerations of the two adsorptive electrode batch unit of the ECPP were derived and analysed on the basis of the propterties of each single electrode separately.

Nomenclature

a_0^-, a_0^+, a^-, a^+	ionic activities at the inlet and outlet solutions.
c_1, c_2	specific double layer capacities of electrodes 1 and 2 (μF g^{-1})
C_e	specific cell capacitance (μF g^{-1})
C	solution concentration (mol cm^{-3})
E_1, E_2	potential of electrodes 1 and 2 versus a reference electrode
ΔE	potential difference between the two electrodes (V)
E_0	potential attained by the electrodes after short-circuiting
F	Faraday constant
g_1, g_2	weights of electrodes 1 and 2 (g)
i	denotes electrode 1 or 2 in a two electrode system
K	dielectric constant of the solution at the double layer region
Δn_S	change in salt content in the solution in one electrode system (moles)
$\Delta n^+, \Delta n^-$	total amount of adsorbed cations and anions in one electrode system (moles)
n_s^t	total amount of salt adsorbed on the electrodes (moles)
n_s	amount of salt adsorbed per unit weight of electrode material (moles g^{-1})
n_i^-, n_i^+	amount of anions and cations adsorbed on unit weight of electrode i (where $i = 1, 2$) (mol g^{-1})
Δq	the change in total electrode charge in one electrode system (C)
q_i	total charge per unit weight of electrode i (C g^{-1})
q_i^+, q_i^-	cationic and anionic charges per unit weight of electrode i (C g^{-1})
q_e, q_d	independent charge coordinates (C g^{-1})
R	gas constant
T	absolute temperature
w	electrical work of charging the double layer (eV)
ϵ_0	free space permittivity
μ_1, μ_2	relative weights or elelctrode 1 and 2 respectively

0021–891X/83 $03.00 + .12.

1. Introduction

In a previous publication [1], electrochemical parametric pumping (ECPP) was introduced as a new concept in separation science. The parametric pumping process, first proposed by Wilhelm and Sweed [2], and studied further by Pigford *et al.* [3] and Wilhelm *et al.* [4], was extended to electrochemical systems. As a first demonstration of the idea, we chose the desalination of dilute aqueous solutions which, we believe, has some potential advantages over existing non-thermal desalting methods. Desalting by ECPP is carried out be electroadsorption over a couple of high specific surface area carbon electrodes, shaped into a multistage separation column. The basic separation process comprises electrically induced adsorption–desorption cycles of cations and anions on the oppositely charged electrodes. These cycles were synchronized with periodical reversals of axial flow. It was shown that such an operation results in a build-up of an axial concentration gradient [5].

The electroadsorptive properties of a two electrode cell is solely determined by the characteristics of each single electrode, namely by the amount of cation and anion adsorbed (or desorbed) on each electrode as a function of its potential and the solution concentration. They are however electrically linked through the outer electrical circuit in such a way that the amount of electrical charge driven off from one electrode, is delivered to the other.

In the present paper the equilibrium properties of the two electrodes which compose the bed of the desalination ECPP column will be established on the basis of the electrical data of each single electrode. The treatment will clarify some of the basic features of the ECPP column, provide some criteria for the optimization of the column performance and yield the basic data necessary for the quantitative treatment of the ECPP dynamics that will be presented in a subsequent article.

2. Experimental procedure

2.1. *Single electrode studies*

The experimental set-up was described in detail elsewhere [6]. It enabled us to measure point by point the electronic charge and electrical potential of the electrode, the amount of adsorbed cation and anion and the pH of the solution.

A large, high surface area carbon electrode was charged and discharged with a constant current in an aqueous NaCl solution against a large Ag–AgCl counter-electrode in the same solution.

Electroadsorption on the 12 000 cm^2 total electrode area resulted in detectable changes on solution concentration. This was monitored by accurate conductivity measurements. The total amount of cation, Δn^+, and anion, Δn^-, adsorbed on the carbon electrode surface could then be calculated according to the following expressions:

$$\Delta n^+ = \Delta n_S$$

where Δn_S is the change in salt content of the solution and,

$$\Delta n^- = \frac{\Delta q}{F} = \Delta n^+$$

where Δq is the change in electrode charge and F is the Faraday number.

2.2. *Two adsorptive electrode system*

This system was also described in a previous article [1]. It is, in fact, a separation column originally built for ECPP operations, but was frequently operated as a batch unit cell in order to obtain the equilibrium adsorptive properties discussed in this paper. The adsorbing bed of the column consisted of two high-surface carbon electrodes with a porous separator between them. The dimensions of the electrodes were

0.2 x 1 x 90 cm. Conductivity cells attached to the outlets of the column were used to detect concentration variations in the internal solution.

Measurements at equilibrium were performed by galvanostatic charging steps followed by waiting periods until the cell potential reached a constant value. The solution was then pumped out of the column and analysed by means of the adjacent conductivity cells. These measurements yielded data of both cell charge q_e which will be defined later, and the net amount of salt adsorbed, as a function of cell potential difference. The measurements were performed for different concentrations and as a result it was possible to draw isopotentiograms.

The differential electrical double layer capacity of the complete two electrode cell, was obtained as described previously [1], from the limiting slope of the galvanostatic curve. The pH of the effluent was monitored by means of glass electrodes located close to the lower column edge.

Solutions of sodium chloride in a concentration range of 10^{-2} to 0.2 mol dm^{-3} were used. The two identical high surface electrodes were made of 60/10 mesh gas chromatography grade carbon black (Carbopack B by Supelco) which has a specific surface area of 100 $m^2\,g^{-1}$.

3. Results and discussion

In the simplest case of nonspecific adsorption, any increase in the electrode potential would result in an increase in anion adsorption and cation desorption [7]*. An electroadsorptive cell comprising two electrodes is operated by transferring an amount of charge Δq_e from one electrode to the other. Thus while anions are adsorbed on the positively charged electrode, they are desorbed from the second, negatively charged one and vice versa for the cations. This implies that Δn_S, the total amount of salt adsorbed can be less than the charge equivalent, Δq_e passing through the cell. For certain single electrode characteristics and a working potential range the charge efficiency term $F\Delta n_S/\Delta q_e$ can even be zero. It is necessary therefore to derive efficiency parameters and establish the relations between single electrode and whole cell characteristics.

3.1. *Independent charge coordinates*

For a single electrode in an electrolyte solution there is one (electrical) degree of freedom at constant pressure, temperature and solution concentration. For convenience let us choose the electrode double layer charge q as the independent variable allowing the potential to receive the appropriate value. The zero of the charge scale on the charge–potential diagram can be set arbitrarily (unless some definite thermodynamic relations [9, 10] or molecular models [11] are involved). For instance we may choose $q = 0$ when the electrode potential is zero versus the familiar Ag–AgCl electrode in the same solution. In a two adsorptive electrode cell, there should be two degrees of freedom. Let these be q_1 and q_2, i.e., the double layer charges per gram of the electrode material of the first and the second electrode respectively, with regard to the same arbitrary zero reference. Since these two charge values are interdependent due to the electrodes connection to the power supply new charge coordinates, q_d and q_e, which can be varied independently, may be defined. These are:

$$q_d = \mu_1 q_1 + \mu_2 q_2 \tag{1}$$

$$2q_e = \mu_1 q_1 - \mu_2 q_2 \tag{2}$$

where:

$$\mu_1 = \frac{g_1}{g_1 + g_2} \tag{3a}$$

$$\mu_2 = \frac{g_2}{g_1 + g_2} \tag{3b}$$

* In cases of strong specific adsorption of anions for instance, anion concentration increases more than the electrode charge and is electroneutralized therefore by increasing cation adsorption even at exceedingly positive potentials [8].

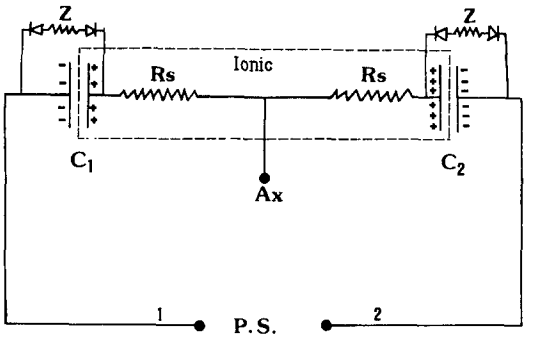

Fig. 1. Equivalent electrical circuit of a two adsorptive electrodes cell. R_s, solution resistance between the two electrodes; C_1 and C_2, electrical double layer capacitors; 1 and 2, the electrodes' connections to the power supply PS. A_x, an auxilliary electrode, Z, a Zener diode.

where g_1 and g_2 are the weights of the first and second electrodes, respectively. The significance and independence of q_d and q_e is best demonstrated by means of the simplified equivalent circuit depicted in Fig. 1. The capacitors C_1 and C_2 represent the electrical double layers of the two electrodes while R_s is the resistance of the solution. The dashed line encloses the solution side of the cell. The capacitors may be unequal in magnitude and potential dependent. The Zener diodes Z represent electrochemical reactions which enable the passage of (Faradaic) current only if the cell potential exceeds the double layer potential range. The electrode charges, g_1q_1 and g_2q_2, are considered positive when the metallic side of the double layer is charged positively. As demonstrated in Fig. 1, the solution side of the double layer of electrode 1 is charged with +4 coulombs and electrode 2 with +6 coulombs. Hence from Equation 1 $(g_1+g_2)q_d = +10$ coulombs, q_d is therefore the total (ionic) charge per gram of total electrode material in the cell entrapped at the solution side of both double layers. It can be seen from Fig. 1 that q_d cannot be changed by passing a current through the leads 1 and 2 of the adsorptive electrodes; q_d can be changed only by means of a third electrode, Ax. This can be explicitly proved if we recall that electroneutrality considerations require that only equal and opposite charges can be passed through the electrodes 1 and 2, thus,

$$g_1\,dq_1 = -g_2\,dq_2 \tag{4}$$

Using Equations 3a and 3b, the complete differential of Equation 1 can be written as follows:

$$(g_1+g_2)\,dq_d = g_1\,dq_1 + g_2\,dq_2$$

combining the latter expression with Equation 4 we obtain $dq_d = 0$. For further elucidation of the meaning of q_e, Equations 1 and 2 are combined to obtain:

$$2q_e = 2\mu_1 q_1 - q_d. \tag{5a}$$

By differentiating at constant q_d, we get:

$$dq_e = \mu_1\,dq_1. \tag{5b}$$

The subtraction of Equation 1 from Equation 2 gives:

$$2q_e = q_d - 2\mu_2 q_2. \tag{6a}$$

Again, for constant q_d we get:

$$dq_e = -\mu_2\,dq_2 \tag{6b}$$

It turns out that $(g_1+g_2)\,dq_e$ is simply the total charge passed between electrodes 1 and 2 by means of a power supply. Its zero value corresponds, according to Equation 2, to a state of equal charges $g_1q_1 = g_2q_2$ of the separate electrodes. Furthermore, q_e may be varied independently on q_d.

3.2. *Criteria for the desalination efficiency and capacity*

The salt adsorption capacity per gram of electrode material of the cell depends on the specific surface area of the electrode and on the electrical variables (potential or charge). Since a third electrode (like Ax shown in Fig. 1) is not likely to be used in a practical desalination setup, q_d is taken as constant and the charge q_e will be the single electrode variable of the cell. The differential charge efficiency of the desalting cell will be defined as: $F(\partial n_s/\partial q_e)_{q_d}$; n_s is determined by the expression:

$$n_s = \frac{n_s^t}{g_1 + g_2}$$

where n_s^t is the total amount of salt adsorbed on the electrodes.

The average charge efficiency for predetermined variations of the charge q_e during the charging step of the ECPP from q_{e1} to q_{e2} is given by:

$$F\frac{\Delta n_s}{\Delta q_e} = \frac{1}{q_{e2} - q_{e1}} \int_{q_{e1}}^{q_{e2}} \frac{\partial n_s}{\partial q_e} \, dq_e. \tag{7a}$$

The differential adsorption energy efficiency of the complete cell is defined as $F(\partial n_s/\partial w)_{q_d}$, where w is the electrical work of charging the double layer, namely:

$$dw = \Delta E \, dq_e = \frac{q_e}{C_e} dq_e. \tag{7b}$$

$\Delta E = E_2 - E_1$ is the potential difference across the cell terminals (E_1 and E_2 are the potentials of electrode 1 and 2 respectively) and C_e is the cell double layer specific capacitance.

Thus,

$$F\left(\frac{\partial n_s}{\partial w}\right)_{q_d} = \frac{C_e}{q_e}\left(\frac{\partial n_s}{\partial q_e}\right)_{q_d}. \tag{7c}$$

The adsorption energy efficiency expressed in Equation 7c is the differential electrical energy invested during a charging step*. It is normalized in such a way that it becomes unity if 1 eV is required for the removal of one molecule of univalent salt from the solution.

A second energy efficiency criterion could be based on the thermodynamic free energy of desalination, which amounts to $n^- RT \ln a_O^-/a_I^- + n^+ RT \ln a_I^+/a_O^+$, where n^- and n^+ are respectively the number of moles of the negative and positive ions adsorbed on the electrodes and a_I^-, a_I^+, a_O^- and a_O^+ are respectively the corresponding activities of the ions in the solution at the outlet and the inlet of the cell. This criterion is of limited importance since the real energy investment is considerably greater and is much more closely related to the energy stored at the double layer capacitance than to the theoretical thermodynamic work.

At high charging and discharging rates, the real energy efficiency is considerably lower than the equilibrium value expressed by Equation 7c because of the high resistive losses. The equilibrium energy efficiency is therefore relevant only at low rates which prevail whenever energy saving is a major optimization factor. On the other hand, when highest desalting yield (thus highest cycling rate) is more important, charge efficiency becomes the more relevant criterion. These two efficiency values provide, therefore, a range of operating conditions within which the optimum should fall.

In the following sections, the detailed derivation of energy and charge efficiencies of a two electrode cell by means of single electrode data will be presented. Also the range of q_d and q_e where these efficiencies attain their highest values will be discussed.

* In principle this energy could at least be partially recovered during the discharge if the power supply is capable of receiving d.c. energy at variable potentials. Alternatively, cycle phase differences between column stacks could be programmed to allow mutual energy transfer.

3.3. Derivation of the differential charge efficiency

Due to the electroneutrality of the solution, an increment in the amount of salt adsorbed is equal to the increment in the amount of anions adsorbed at both electrodes and is the same as that of cation adsorbed at both electrodes and is the same as that of cation adsorbed at both electrodes, namely,

$$(g_1+g_2)\mathrm{d}n_s = g_1\mathrm{d}n_1^- + g_2\mathrm{d}n_2^- = g_1\mathrm{d}n_1^+ + g_2\mathrm{d}n_2^+ \tag{8}$$

n_1^-, n_2^-, n_1^+ and n_2^+ are respectively the number of equivalents of anions and cations adsorbed on electrodes 1 and 2 per gram of electrode material. Differentiating with respect to q_e at constant q_d and using Equations 5b, 6b, 3a and 3b we get:

$$\left(\frac{\partial n_s}{\partial q_e}\right)_{q_d} = \frac{\partial n_1^-}{\partial q_1} - \frac{\partial n_2^-}{\partial q_2} = \frac{\partial n_1^+}{\partial q_1} - \frac{\partial n_2^+}{\partial q_2}. \tag{9}$$

Multiplying Equation 9 by F and denoting Fn^- and Fn^+ by q^- and q^+ respectively, we obtain:

$$F\left(\frac{\partial n_s}{\partial q_e}\right)_{q_d} = \frac{\partial q_1^-}{\partial q_1} - \frac{\partial q_2^-}{\partial q_2} = \frac{\partial q_1^+}{\partial q_1} - \frac{\partial q_2^+}{\partial q_2} \tag{10}$$

which is the differential charge efficiency expressed in terms of *single electrode* ion adsorption efficiencies.

It is noteworthy that the present work deals with the equilibrium adsorptive properties of the complete two electrode cell as a superposition of single electrode characteristics. This is basically different from the previous work by Johnson and Newman [13] which dealt with the transient behaviour of a single electrode of the desalination cell.

The electroneutrality condition of the double layer of electrode i ($i = 1$ or 2) is:

$$\mathrm{d}q_i^- = \mathrm{d}q_i - \mathrm{d}q_i^+ \tag{11}$$

where q_i is the total charge per gram of electrode i. This condition converts the second equality of Equation 10 to an identity. Equation 10 shows that the amount of salt adsorbed by the two electrodes is not necessarily equivalent to the charge q_e passed and can even be zero when $\partial q_1^-/\partial q_1 = \partial q_2^-/\partial q_2$. Therefore, a brief survey of the relevant aspects of adsorption at the electrical double layer of electrodes is needed in order to find out the conditions of maximum salt adsorption. If no specific adsorption occurs, anions and cations of a Z–Z electrolyte behave almost symmetrically. The implications of this are as follows:

If both electrodes were located at the potential of zero charge PZC, then,

$$\frac{\partial q_1^-}{\partial q_1} = \frac{\partial q_2^-}{\partial q_2} = \frac{1}{2} \tag{12}$$

and the charge efficiency (Equation 10) vanishes.

For extreme positive potentials the double layer is depleted of cations over a significant potential range. Therefore, $\partial q_i^+/\partial q_i$ vanishes. By mean of the electroneutrality condition (Equation 11) we obtain,

$$\frac{\partial q_i^+}{\partial q_i} + \frac{\partial q_i^-}{\partial q_i} = 1 \tag{13}$$

If $\partial q_i^+/\partial q_i$ is very small, $\partial q_i^-/\partial q_i$ approaches unity. The opposite applies to extreme negative potentials. If electrodes 1 and 2 were made extremely positive and extremely negative respectively, the above approximations read:

$$\frac{\partial q_1^+}{\partial q_1} \approx 0; \quad \frac{\partial q_1^-}{\partial q_1} \approx 1; \quad \frac{\partial q_2^+}{\partial q_2} \approx 1; \quad \frac{\partial q_2^-}{\partial q_2} \approx 0$$

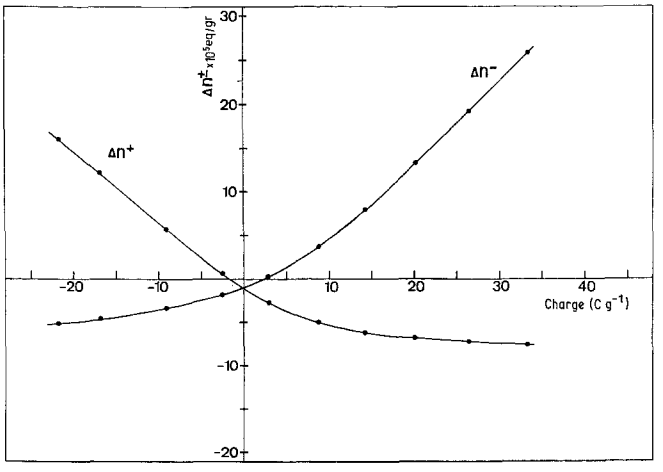

Fig. 2. Typical anion and cation adsorption curves on a single FC-12 electrode. NaCl 0.12 mol dm^{-3} solution.

By inserting these limiting values in Equation 10 a unit charge efficiency is yielded. The two electrode cell should therefore approach its highest capacity upon keeping the electrodes at extreme and opposite q_i values.

In these circumstances $\partial q_1^-/\partial q_e$ and $\partial q_2^-/\partial q_e$ are unity and zero respectively, provided electrode 1 is positively charged. Consequently the differential charge efficiency becomes unity. Non-specific adsorption is quite an abundant case and occurs on many metals such as mercury with NaF solution [8]. These properties are also among the consequences of the Gouy–Chapman–Stern (GCS) model for non specific adsorption on electrodes [14]. Adsorption of sodium and chloride ions on FC-12 carbon electrodes was also shown to be essentially non-specific [7]. For this system, typical curves of cation and anion adsorption versus electrode charge are given in Fig. 2, and the corresponding slope $\partial q^-/\partial q$ is given in Fig. 3. The symmetry of the anion and cation curves in Fig. 2 is noteworthy. In Fig. 3 are also given some values from mercury electrodes at similar conditions. Data on mercury were calculated from curves of q^-, q^+ and q versus the electrode potential as measured by Grahame and Soderberg [8].

At higher bulk concentrations the concentration of ions bearing the same charge sign as that of the electrode at the double layer region is also higher, therefore its depletion from the double layer is more difficult. The approach of the slopes of the adsorption–charge curves to zero and unity at extremely large positive and negative charges is thus less likely. The consequence regarding Equation 10 is that the charge efficiency may be lower for higher concentrations. This does occur in fact on a single

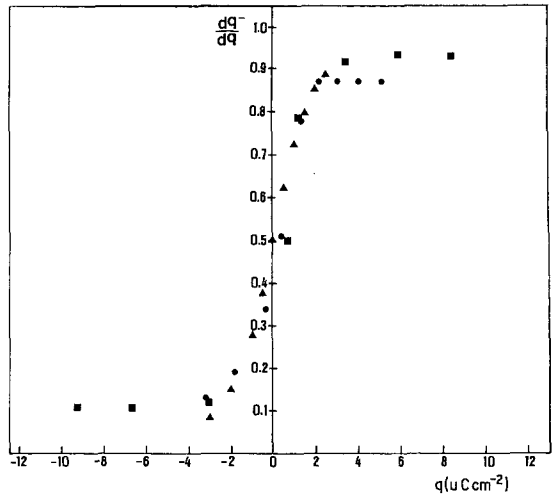

Fig. 3. Typical slopes $\partial q^-/\partial q$ against electrode charge q. ▲ FC-12 carbon electrodes; ● GCS model with $K = 20$; ■ KF solution on a mercury electrode [8].

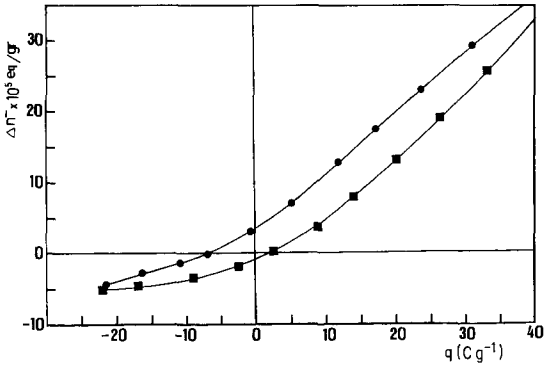

Fig. 4. Anion adsorption curves on FC-12 carbon for two NaCl concentrations. ■, 0.12 mol dm^{-3}; ●, 0.67 mol dm^{-3}.

FC-12 electrode as shown in Fig. 4. The effect on charge efficiency of the complete cell is demonstrated in the Fig. 5 by the family of curves of salt adsorbed as a function of q_e. It is evident from this figure that the slope $\partial n_s/\partial q_e$ decreases with increasing solution concentration.

Considering the behaviour of the non-specific adsorbing electrodes described above, it can be concluded that the adsorption efficiency expressed in Equation 10 cannot exceed unity. This may occur, however, in cases of strong specific adsorption which is very frequently found on metallic surfaces with high halogens [8].

The differential charge efficiency $\partial n_s/\partial q_e$ can be calculated from the single electrode properties according to Equation 10 if an explicit function of $\partial q_i^{\pm}/\partial q_i$ is known from a model; otherwise it can be evaluated graphically by means of experimental curves of $\partial q_1^-/\partial q_i$ against the electrode charge or potential.

3.4. *Calculation of* $\partial n_s/\partial q_e$ *according to the GCS model*

The GCS model refers only to the potential drop between the outer Helmholtz plane and the bulk of the solution [15]. We shall express $\partial n_s/\partial q_e$ as a function of q and q^- according to this model. These magnitudes will later be linked to the electrode potential by means of experimental charge–potential curves.

The single electrode components $\partial q^-/\partial q$ in Equation 10 as given by the GCS theory [16] are:

$$\frac{\partial q^-}{\partial q} = \frac{1}{2}\left\{1 + \frac{q/2A}{[(q/2A)^2 + 1]^{1/2}}\right\} \tag{14}$$

where

$$A = (2RTK\epsilon_0 C)^{1/2} \tag{15}$$

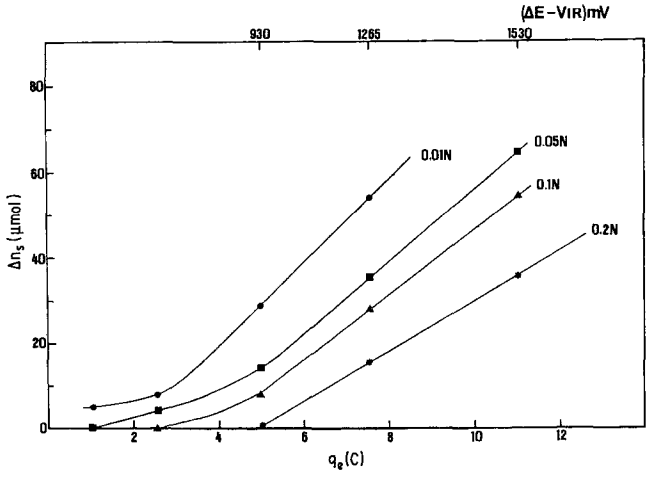

Fig. 5. Total amount of salt adsorbed in the two electrodes cell against change of electrode charge.

where K is the dielectric constant, ϵ_0 the free space permittivity and C the solution concentration in moles cm^{-3}.

One can deduce from Fig. 3 that Equation 14 satisfactorily fits the experimental curve for the FC-12 carbon, if $K = 20$*. Introducing Equation 14 in Equation 10 for each electrode, using the dimensionless charge units:

$$Q_e = \frac{q_e}{2A} \qquad \text{and} \qquad Q_d = \frac{q_d}{2A} \tag{16}$$

and Equations 5a and 5b, the expression:

$$F\left(\frac{\partial n_s}{\partial q_e}\right)_{q_d} = \frac{1}{2}\left\{\frac{Q_e + (Q_d/2)}{[(Q_e + Q_d/2)^2 + \mu_1^2]^{1/2}} + \frac{Q_e - (Q_d/2)}{[(Q_d/2 - Q_e)^2 + \mu_2^2]^{1/2}}\right\} \tag{17}$$

is obtained.

It is noteworthy that once the GCS model has been introduced, the zero values of q_1, q_2 and q_d are no longer arbitrary and refer to the potential of zero charge [9, 18]. Equation 17 has an even symmetry with respect to Q_d and an odd symmetry with respect to Q_e.

The differential charge efficiency calculated from Equation 17 is depicted in Fig. 6 as a function of the dimensionless charge Q_e, for different Q_d values. It is evident that the efficiency is higher as Q_d decreases. Considering Equation 7a, the optimal range of q_e can also be deduced from Fig. 6 by means of expression 16 for Q_e. The lower limit, q_{e1}, should be somewhat above zero while the higher limit, q_{e2}, has to be as large as possible, if only charge efficiency is accounted for. It is obvious, however, that q_{e2} may practically be increased only to a limit set by Faradaic processes such as water electrolysis. Furthermore, as will be deduced subsequently, energy efficiency considerations set further limits to q_{e1} and q_{e2}. The regions of very low efficiency for combinations of high $|Q_d|$ and low $|Q_e|$ values are due to the fact that under such conditions both electrodes are highly charged on the same side of the zero value; hence $\partial q_1^-/\partial q_1$ and $\partial q_2^-/\partial q_2$ of the single electrodes approach unity and the charge efficiency as given in Equation 10 becomes small. This feature can be predicted by the more general assumptions of symmetrical behaviour of cations and anions at the double layer.

A family of curves of charge efficiency against the cell variable q_e for different constant values of q_d (like those of Fig. 6) could also be formed one the basis of purely experimental data of the single electrodes. This is done as follows: the experimental $\partial q_1^-/\partial q_1$ and $\partial q_2^-/\partial q_2$ plotted on the q_1 and q_2 abscissas, respectively, are both transformed into the q_e abscissa for a commonly selected q_d. The difference $\partial q_1^-/\partial q_1 - \partial q_2^-/\partial q_2$ is then picked up point by point as a function of q_e calculated by means of Equation 2 with the appropriate values of q_1 and q_2. According to Equation 10, these points should provide the corresponding $F(\partial n_s/\partial q_e)$ versus q_e curve for the selected q_d. One can, furthermore, deduce from Equations 5a and 6a that a different choice of q_d value would result in just symmetrical and opposite shifts of each of the $\partial q_1^-/\partial q_1$ and $\partial q_2^-/\partial q_2$ versus q_e curves by $\Delta q_d/2$, where Δq_d is the difference between the q_d selections. This procedure by no means requires two identical electrodes for the desalination cell. However, in the case of non-specific adsorptive electrodes, the symmetrical behaviour

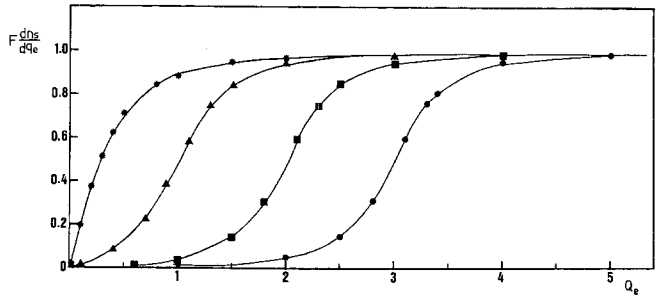

Fig. 6. Theoretical differential charge efficiency calculated from Equation 17. Q_d: *, −0; ▲, −2; ■, −4; ●, −6.

* K for the 'electrified interface' is considered lower than that of bulk water because of partial dielectric saturation [17].

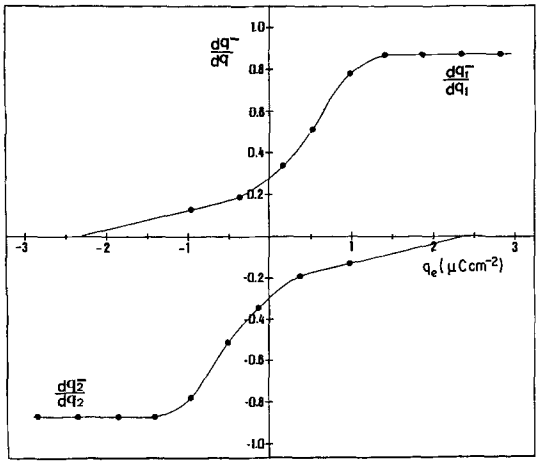

Fig. 7 $\partial q_1^-/\partial q_1$ and $\partial q_2^-/\partial q_2$ as a function of q_e for a simulated symmetrical cell composed of two FC-12 electrodes, $q_d = 0.65\ \mu C\ cm^{-2}$.

towards anion and cation adsorption leads to identical electrodes of equal weights as the best choice. Figure 7 shows experimental curves of $\partial q_1^-/\partial q_1$ and $\partial q_2^-/\partial q_2$ versus q_e obtained from data of Fig. 4 for a symmetrical cell composed of two FC-12 electrodes. The chosen value of q_d corresponded to that of an electrode at a potential of 20 mV versus SCE, this is to say that for $q_e = 0$ both electrodes are at this potential.

The differential charge efficiency, measured directly from the complete cell packed with two symmetrical Carbopack B carbon electrodes, can now be compared with that composed of single (FC-12) electrode data (by integration of Equation 10). This comparison is done in Fig. 8. One should not expect to find a perfect correspondence between the two curves since two different electrode materials (having different adsorption characteristics) are used in the single electrode and complete cell system.

The fact that the complete cell efficiency curve levels off at high q_e values may be due to the following: at extreme q_e values, part of the charge is consumed by electrochemical processes which involve water rather than salt ions and thereby lower the pH upon positive charging and raise it upon negative charging [7]. This effect reduces the ion charge efficiencies $\partial q_i^-/\partial q_i$ and $\partial q_i^+/\partial q_i$ and was found to become more significant as the charge becomes larger. For elementary thermodynamic reasons the pH changes in the single electrode system should impede the processes which involve water. In the two electrode system it was found that the pH remained almost neutral presumably as a consequence of mutual buffering of the oppositely charged electrodes. There is therefore less impediment of the processes involving water in the complete cell. That may lead to a lower charge efficiency for the real

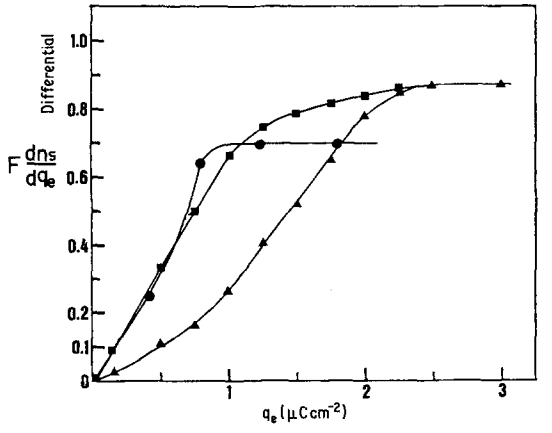

Fig. 8. Differential charge efficiencies deduced from Fig. 7 (■ $q_d = 0.65\ \mu C\ cm^{-2}$; ▲, $q_d = 2.6\ \mu C\ cm^{-2}$) compared to the two electrodes system, ●.

two electrode system as compared to values calculated from single electrode data. This is indeed shown in Fig. 8.

In light of these considerations we may regard the approximate fit between the charge efficiency curve for the complete cell and those calculated from single electrode data as quite satisfactory.

3.5. *Adsorption energy efficiency*

As noted in Section 3.2, this criterion may be preferable whenever energy economy is of main importance. It will be treated here in a similar way as the absorption charge efficiency.

In order to apply the GCS model, Equation 17 is substituted into Equation 7c to obtain the following dimensionless equation for the adsorption energy efficiency:

$$\frac{4AF}{C_e}\left(\frac{\partial n_s}{\partial w}\right)_{q_d} = \frac{1}{Q_e}\left\{\frac{Q_e+(Q_d/2)}{[(Q_e+Q_d/2)^2+\mu_1^2]^{1/2}}+\frac{Q_e-(Q_d/2)}{[(Q_d/2-Q_e)^2+\mu_2^2]^{1/2}}\right\}. \tag{18}$$

The left hand side of this equation is plotted in Fig. 9 for different Q_d values. Unlike the adsorption charge efficiency presented in Fig. 6, the adsorption energy efficiency drops for high q_e values and acquires maxima for intermediate q_e values. This is undoubtedly due to the square power dependence of the capacitor energy with charge while ion adsorption is at most proportional to charge. As in the case of charge efficiency, the optimal value of the energy efficiency is obtained when Q_d is zero. The best q_{e1} is thus also zero, whereas charge efficiency considerations lead to a different value. Further more, unless a lower limit is preferred to prevent the electrochemical decomposition of the solution, the best values for q_{e2} are set at the points of maximum energy efficiency.

As in the case of charge efficiency, a purely empirical procedure may be forwarded to obtain the adsorption energy efficiency from the single electrode experimental data. By substitution of Equation 10 into Equation 7c, we obtain:

$$F\left(\frac{\partial n_s}{\partial w}\right)_{q_d} = \frac{C_e}{q_e}\left(\frac{\partial q_1^-}{\partial q_1}-\frac{\partial q_2^-}{\partial q_2}\right). \tag{19}$$

Now $C_e = (\partial q_e/\partial(E_1-E_2))_{q_d}$ is the specific cell capacitance and $(g_1+g_2)C_e$ is the whole cell capacitance. We can therefore write:

$$\frac{1}{C_e} = \left(\frac{\partial(E_1-E_2)}{\partial q_e}\right)_{q_d} = \left(\frac{\partial E_1}{\partial q_e}\right)_{q_d} - \left(\frac{\partial E_2}{q_e}\right)_{q_d}. \tag{20}$$

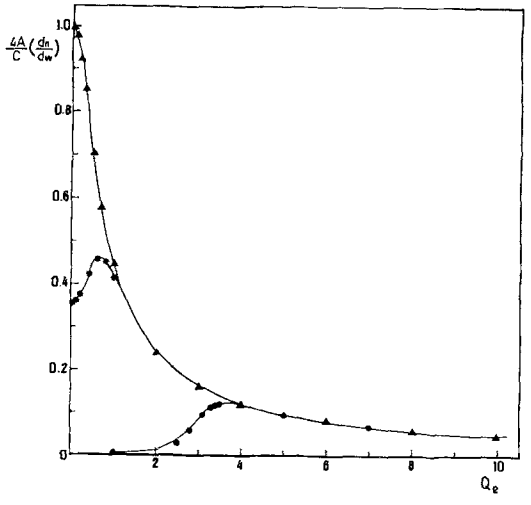

Fig. 9. Theoretical energy efficiency against Q_e for different values of Q_d: ▲, −0; ∗, −1; ●, −6.

Using Equations 5b and 6b we obtain:

$$\frac{1}{C_e} = \frac{1}{\mu_1}\left(\frac{\partial E_1}{\partial q_1}\right)_{q_d} + \frac{1}{\mu_2}\left(\frac{\partial E_2}{\partial q_2}\right)_{q_d} = \frac{1}{\mu_1 c_1} + \frac{1}{\mu_2 c_2}. \tag{21}$$

This shows that C_e results from a series connection of the two electrode specific capacitances c_1 and c_2. Combination of Equations 21 and 19 gives:

$$F\left(\frac{\partial n_s}{\partial w}\right)_{q_d} = \frac{1}{q_e}\left(\frac{\partial q_1^-}{\partial q_1} - \frac{\partial q_2^-}{\partial q_2}\right)\left(\frac{1}{\mu_1}\frac{\partial E_1}{\partial q_1} + \frac{1}{\mu_2}\frac{\partial E_2}{\partial q_2}\right)^{-1}. \tag{22}$$

Hence, to find $F(\partial n_s/\partial w)$ we must resort the graphical computation of the denominator $1/C_e$ of Equation 22 in the same way shown earlier for the numerator (Equation 10). This will provide a family of curves of $1/C_e$ versus q_e for constant q_d. Then, the family of curves of $F(\partial n_s/\partial w)$ will be obtained by the corresponding division of the known values of Equation 22.

The above procedure becomes much simpler if it is assumed that the specific capacitances c_1 and c_2 of the single electrodes are constant and equal to c thus, according to Equation 21 $C_e = c\mu_1\mu_2$. This is, in fact, a good approximation for carbon electrodes [6, 19] over a wide concentration range [20], as well as for other electrodes in the case of non-specific adsorption conditions and considerable concentrations [21]. In this work the complete cell capacitance was directly measured for different concentrations and found to change over the whole potential range by 30% as shown in Table 1. For a first approximation, an average constant c may be justified so that the direct application of Equation 19 instead of Equation 22 is possible. Fig. 10 depicts the differential energy efficiency calculated by means of Equation 19 for a cell composed to two FC-12 electrodes using single electrode data and by means of Equation 7c for the complete cell packed with two Carbopack B electrodes. As in the theoretical curves shown in Fig. 9, these curves also show a maximum. Although the maximum appears for the same q_e magnitude as for the single electrode model, the whole efficiency curve is about 2.8 times lower. Bearing in mind that the corresponding charge efficiency curves fit quite well (Fig. 8) the disagreement in Fig. 10 should be attributed mainly to a difference in the double layer capacities c exhibited by the different electrodes (3.4 times greater for FC-12 electrodes).

3.6. *Adjustment of* q_d

It has been shown above that the value of q_d has a crucial influence on the efficiency of the electro-adsorption cell. Adjustment of q_d is possible only by means of a third electrode (cf. Fig. 1) which, in

Table 1. Complete cell double layer capacitance at various potentials and concentrations

ΔE (mV)	*Specific cell capacitance,* C_e ($\mu F\,cm^{-2}$)			
	Concentration 0.2 mol dm^{-3}	*Concentration* 0.1 mol dm^{-3}	*Concentration* 0.05 mol dm^{-3}	*Concentration* 0.01 mol dm^{-3}*
200	4.84	3.80	3.44	3.09
400	4.84	3.96	3.44	3.48
600	4.33	4.15	4.19	3.69
800	4.55	4.65	4.15	4.45
1000	5.47	4.84	5.42	4.62
1200	5.66	5.42	5.42	4.74
1400	6.1	6.45	6.33	5.03
1600	6.1	6.45	6.33	–

* Corrected for IR drop.

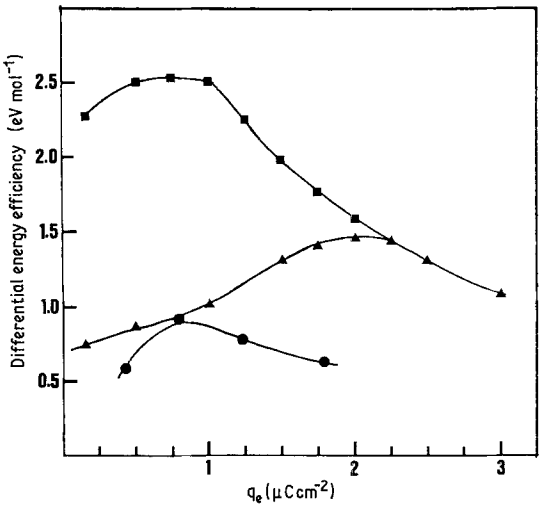

Fig. 10. Experimental differential energy efficiencies for simulated FC-12 electrodes cell (■, $q_d = 0.65\ \mu C\,cm^{-2}$; ▲, $q_d = 2.6\ \mu C\,cm^{-2}$) compared to the two electrodes system, ●.

the case of the multistage column, should extend along it [1]. This might considerably complicate the column structure design. In this work, self-adjustment of q_d to its optimal value, which is close to the zero charge, can be achieved by utilizing the charge transfer processes at the margins of the double layer potential range. As was shown in the earlier study of the single FC-12 electrode [6] in neutral NaCl solutions, the potential of zero charge of this electrode falls at about the same distance from the two Nernst potentials of water decomposition. In the equivalent circuit of Fig. 1 the charge transfer across each electrode interface is represented by back to back Zener diodes with breakdown potentials E_c and E_a for cathodic and anodic currents, respectively. A prolonged passage of current through the cell, from electrode 1 to electrode 2, will charge the cathode and anode up to $E_1 c_1$ and $E_2 c_2\,C\,g^{-1}$ respectively. The net charge q_d on both solution sides of the double layer, i.e., between the two capacitors shown in Fig. 1, will then be: $E_1 c_1 - E_2 c_2$. If afterwards the two electrodes are short-circuited (i.e., discharged back to $q_e = 0$), a potential E_0 will be attained by both electrodes, but the charge q_d entrapped between the two electrodes remains constant. Thus, we get

$$E_1 c_1 - E_2 c_2 = E_0(c_1 + c_2) \tag{23}$$

and in the case of a symmetrical cell $c_1 = c_2$, this equation becomes:

$$E_0 = \frac{E_1 - E_2}{2} \tag{24}$$

which, as already stated, is the position which determined the optimal q_d. In conclusion, a slight overcharge of the cell during the charging step of the ECPP will always keep q_d constant and reproducible so that the potential E_0 of the two electrodes for $q_e = 0$ will obey Equation 24. No third electrode would consequently be necessary for this adjustment.

The above derived value of E_0 does not necessarily provide the best q_d values for all carbon electrodes since different carbons vary in their surface oxidation states and therefore also in their potential of zero charge [20]. However, we have found that the Carbopack B carbon used in the ECPP column exhibits the lowest charge efficiencies for $\Delta E = 0$, namely when both electrodes are at E_0. This can be recognized by observing that the slopes of n_s against q_e curves shown in Fig. 5 for various constant concentrations, becomes smaller as the potential difference between the electrodes decreases.

3.7. *The isopotentiogram*

The two electrode cell should be considered as a separation device based on the selectivity of a solid adsorbent in contact with a fluid mixture. In the present study, the solid adsorbent is represented by

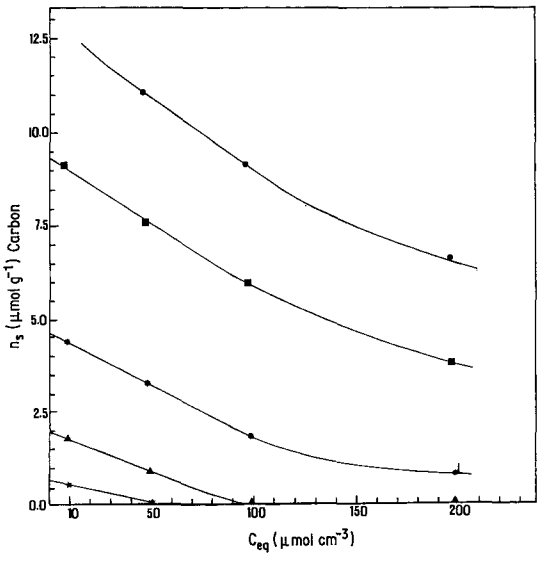

Fig. 11. Amount of salt adsorbed as a function of solution concentration at constant cell potential differences (isopotentiograms). Values of IR drop corrected potentials, $E - V_{IR}$ are: ★, 360 mV; ▲, 600 mV; ✱, 900 mV, ■, 1280 mV; ●, 1550 mV.

the two adsorptive electrodes which are interrelated by Equations 1, 2 and 8. One should therefore anticipate an equivalent to the adsorption isotherm i.e., a dependence of the amount of salt adsorbed on the solution concentration while other intensive variables are kept constant. It will be shown in the following paper [22] that the adsorption functions are of ultimate importance of analysing the dynamics of the ECPP. In addition to the constant T and P, one electrical variable should be kept constant. In this work we sought the highest possible adsorption capacity that would lead to $E_1 - E_2$ values limited only by water electrolysis. The isopotentiogram i.e., isotherms at constant potential difference ΔE is the appropriate function since this work involved charging steps up to a constant ΔE. A series of isopotentiograms obtained from adsorption data for the complete cell is given in Fig. 11. A marked feature which greatly simplified the dynamics of the ECPP is that the vertical spacing $(\partial n_s/\partial \Delta E)$ between the curves is independent of concentration. This behaviour is in agreement with the properties of the double layer on non-specific adsorptive electrodes. We can write:

$$\left(\frac{\partial n_s}{\partial q_e}\right)_{q_d} = \frac{1}{C_e}\left(\frac{\partial n_s}{\partial \Delta E}\right)_{q_d} \tag{25}$$

The complete cell capacitance C_e was shown (Table 1) to be approximately independent of the concentration over a wide potential range. Also $(\partial n_s/\partial q_e)$ was shown to approach unity independently of the concentration, at potentials remote from the PZC (Figs 5 and 7). Hence $(\partial n_s/\partial \Delta E)$ should be concentration independent as well.

4. Concluding remarks

Starting from some physiochemical features of the electrical double layer of an electrode in electrolyte solution, the equilibrium properties of a desalination cell operated by electroadsorption on high specific surface area electrodes were established. These equilibrium properties provide the theoretical background and basic experimental data necessary for studying and understanding the dynamics of a multistage desalination column, whose bed is formed of two electroadsorbing electrodes performing as an electrochemical parametric pump.

References

[1] Y. Oren and A. Soffer, *J. Electrochem. Soc.* **125** (1978) 869.
[2] R. H. Wilhelm and N. H. Sweed, *Science* **159** (1968) 522.
[3] R. L. Pigford, B. Baker III and D. E. Blum; *I. EC. Fundam.* 8 (1969) 144.
[4] R. H. Wilhelm, A. W. Rice and A. R. Bendelius, *Ind. Eng. Chem.* **5** (1969) 144.
[5] R. G. Rice, *Sep. Purif. Methods* **5** (1976) 139.
[6] A. Soffer, Ph.D. thesis, Israel Institute of Technology, Haifa, Israel (1969).
[7] A Soffer and M. Folman, *J. Electroanal. Chem.* **38** (1972) 25.
[8] D. C. Grahame and B. A. Soderberg, *J. Chem. Phys.* **22** (1954) 449.
[9] A. Soffer, *J. Electroanal. Chem.* **40** (1972) 153.
[10] A. N. Frumkin, O. S. Petrii and B. B. Damaskin, *Electrokhimiya* **6** (1970) 614.
[11] R. Parsons, in 'Modern Aspects of Electrochemistry', Vol. I, (edited by J. O'M. Bockris) Butterworths, London (1954).
[12] J. Th. G. Overbeek, in 'Colloid Science', Vol. 1, (edited by H. R. Kruyt) Elsevier Publishing Company Inc. New York, (1949) p. 194.
[13] A. M. Johnson and J. Newman, *J. Electrochem. Soc.* **118** (1971) 510.
[14] P. Delahay, 'Double Layer and Electrode Kinetics', Interscience Publishers, New York, London, Sydney (1945) p. 55.
[15] *Idem, ibid,* p. 35.
[16] D. M. Mohilner, in 'Electroanalytical Chemistry' (edited by A. J. Bard), Marcel Dekker, New York (1966) p. 304.
[17] D. C. Grahame, *J. Chem. Phys.* **21** (1953) 1054.
[18] S. D. Argade and E. Gileadi, in Electrosorption, (edited by E. Gileadi), Plenum Press, New York (1967).
[19] M. Yaniv and A. Soffer, *J. Electrochem. Soc.* **123** (1976) 506.
[20] H. Tobias, M.Sc. thesis, Ben Gurion University, Beer Sheva, Israel (1979).
[21] D. C. Grahame, M. A. Poth and J. I. Cummings, *JACS* 74 (1952) 4427.
[22] Y. Oren, A. Soffer, *J. Appl. Electrochem.* **13** (1983) 489.